TEM Analysis of Implantation Damage from H and He in Silicon

Christopher Jost
Professor Phil Fraundorf
University of Missouri – St. Louis

The effects of implantation of He and H into silicon wafers are studied using Transmission Electron Microscopy (TEM) experiments. The four samples are He and H implantation alone, He followed by H, and H followed by He. The damage layer has shown repeated dark contrast in both Bright Field and Dark Field imaging conditions, suggesting the contrast is not due to typical diffraction effects and is a result of a damaged lattice. The damage layer shows a texture of overlapping dark circles with diameters typically between 9-18 nm.

Introduction

The study of silicon-on-insulator materials has a long history, dating back as early as 1987[1]. While work was being done on silicon/oxide interfaces[2] and defects from Hydrogen[3] in this time frame, all references to SOI that I found in the literature were based on the Separation by Implantation of Oxygen (SIMOX) method[1][4]. This pattern seems to have continued until about the mid-nineties. The dosages of oxygen implantation (per cm^2) were mostly in the 10^{18} range, as opposed to our 10^{16} range[1][4][5]. In the nineties, other ways of making SOI were being explored: one paper looked at burying a silicon nitride layer as an insulator as well as a silicon oxide[5]; another bonded one silicon wafer with a grown oxide layer to a regular wafer and then abraded away all but a thin film from one[6]. Around 1996-2004, interest was being shown in helium-implantation and co-implantation of helium and hydrogen in the context of bubble formation and SOI production[7][8][9][10][11][12]. By 2006, there seemed to be little activity from microscopy conferences in the way of SOI manufacturing processes and instead focused more on devices[13].

This report focuses on as-implanted specimens that were implanted with different combinations of He and H ions. To characterize the damage layer, we sought to measure the full-width half-maximums and implantation depths. We also attempted to get information on the size scale of the damage in the as-implanted state in hopes of giving insight into what is happening before the annealing process leads to bubbles.

One of the biggest burdens to expanding the use of SOI is the cost involved in producing it. By better understanding the processes involved, we can make them more efficient to ultimately reduce costs. The discovery of the synergistic effects of co-implantation[9] of He and H, for instance, have already acted to bring down the total gas dosages needed for implantation.

Experimental Details

Specimen Preparation:

The cross-sections were prepared by bonding two specimen interfaces with M-Bond 610 epoxy and surrounding them with dummy wafers, making a silicon layer "cake." The curing of the epoxy involved baking at 175 C for two hours. A disc was then cut from a thin slice of the silicon "cake" and polished on both sides. The specimen was then

dimpled and ion milled until it was perforated. The use of thermal cement required heating the specimen up to 135 C; this was done three different times on each specimen.

Specimen Information:

Implants for TEM Analysis

SLOT	MEAN OXIDE LAYER THICKNESS (A)	STANDARD DEVIATION OF OXIDE LAYER THICKNESS (A)	Implant Species	Implant Dose (E16/cm^2)	Implant Energy (keV)
1	1515.3	4.8	HE^+	1	36
2	1510.8	5.0	HE^+ followed by H_2^+	1.0 for HE^+, 0.5 for H_2^+	36 for HE^+, 48 for H_2^+
3	1362.5	6.2	H_2^+	0.5	48
4	1386.0	7.2	H_2^+ followed by He^+	0.5 for H_2^+, 1.0 for HE^+	48 for H_2^+, 36 for HE^+
5			Bonded Pair-donor implanted with conditions for wafer in Slot 2	Implanted donor side of the bonded pair is blue (front side), the handle side is gray (backside)	

Table 1

Table 1 shows the details of the samples used in this analysis. Samples 1 and 4 were bonded together in one cake and samples 2 and 3 were bonded in another so that two interfaces could be seen from one sample.

Imaging Conditions:
The first setup involved orienting the specimen near to the <110> zone of the cross-section, with a large (HREM) objective aperture primarily for the added illumination that it provided. This setup also facilitated lattice fringe imaging in sufficiently thin regions of the cross-section. This setting was of interest here because it provided robust access to a contrast band likely associated with diffuse scattering (channeling reduction) in regions of the interface approaching the implantation end-of-range.

The second setup tilted the specimen to the Bragg condition for the interface (200) reflection. Brightfield/Darkfield pairs were taken with a small (high contrast) objective aperture.

Profile/Background-Model Details:
The images were rotated such that the silicon/oxide interface ran vertically. Average intensity information over the damage layer was taken using the image processing software, ImageJ. A rectangular region of interest is drawn and the software averages the intensity values of a column to give a point along the profile. Once the scale is appropriately set, this measurement gives average intensity as a function of distance across the region of interest (Figure 1). This data was then imported into Excel for analysis. To estimate the contribution the damage layer had on the profile, the points deeper than the End of Range (EOR) and just beyond the oxide/silicon interface were used to find a curve that was used as a background model. The profile data in the damage region was then subtracted from the background model to approximate the contribution the damage layer had on the intensity (Figure 2). This data was then used to calculate the full width half-maximum.

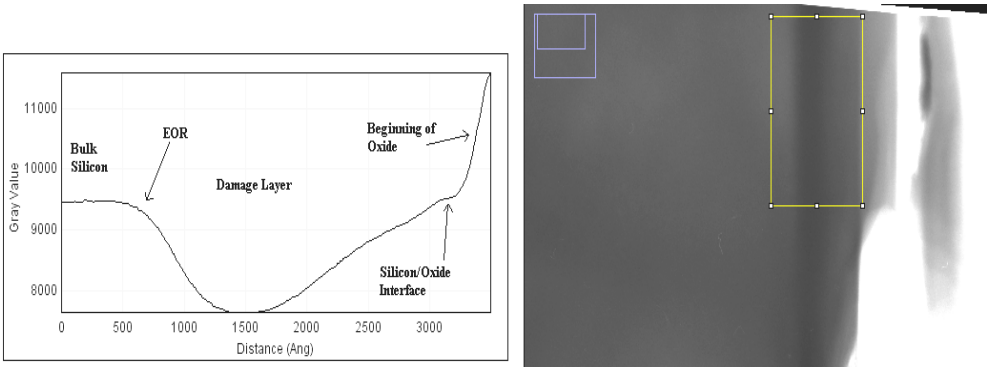

Figure 1

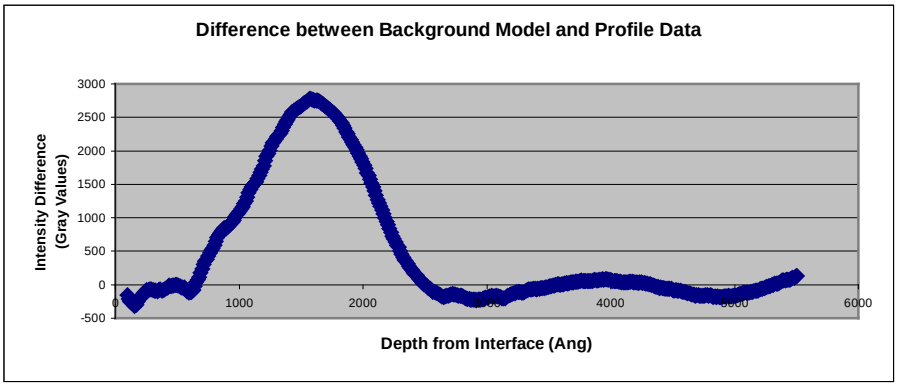

Figure 2

Texture Analysis:

The damage layer had a mottled texture that we wanted to quantify (Figure 3). To do this we took a power spectrum of the damaged region and of a nearby, undamaged region for comparison. We then took the ratio of the radial profiles to see which spatial frequencies the damaged region contained that the healthy silicon did not.

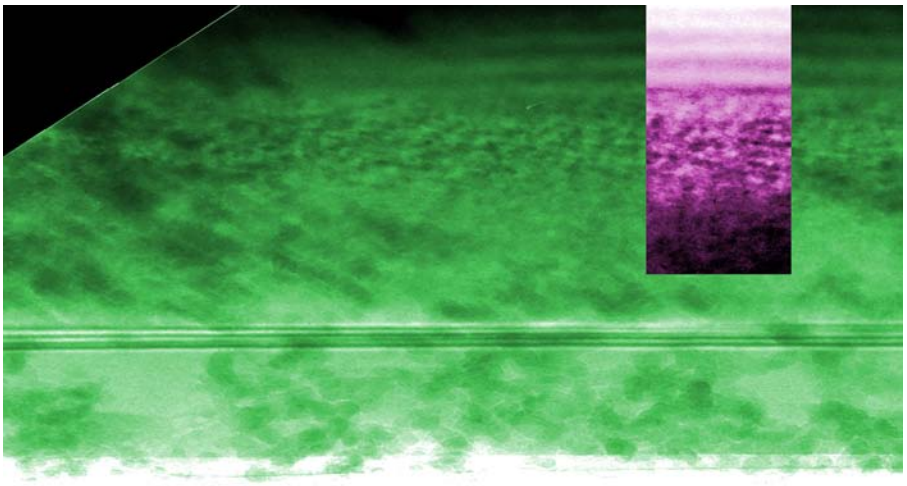

Figure 3

This information was then used to better implement a Digital Darkfield technique. Using *Mathematica*, a mask was created to blackout all frequencies in the power spectrum except for the range of spatial frequencies found by the above process. The inverse-transform is taken of this new power spectrum and only the regions exhibiting the defined spatial frequencies have intensity.

Observations

Contrast:

Before presenting the results of measurements on the images, it is worth discussing what phenomena are causing the contrast we see. First, we observe a dark band parallel to the interface that is near the range we expect the damage from the implantation. Before we recorded images, we were not expecting to see such a prominent band since we expect little contrast from the He and H atoms due to their low atomic number. To our surprise, not only was there a dark band under Brightfield (BF) conditions, but the band was also dark in Darkfield (DF) conditions. The expected complementary contrast in BF/DF image pairs was not observed. This suggests that the scattering process is not due to atoms working together collectively to give diffraction effects, but rather is due to the disruption of Si crystallinity. The displaced Si atoms act to "clog the tunnels" of the symmetry zones in a perfect crystal, giving channeling contrast.

Measurements of depth distributions of displaced atoms due to Helium implantation[10] offer credibility to this interpretation. In specimens implanted with 20 keV He ions at room temperature, the distribution of displaced atoms increases almost linearly until the maximum is reached at about 180 nm, after which is falls off more sharply and ends at about 250 nm. The shape of this curve is qualitatively similar to our intensity vs. depth plots, perpendicular to the damage layer.

Profile Data:

Figure 4 shows a comparison of the damage peaks of all four specimens. The intensity values were multiplied by a constant to give the same maximum so that the shapes of the peaks could be compared. All spatial measurements are in units of Angstroms and the depth is a measurement from the lowest intensity point in the damage layer to the oxide/silicon interface.

Specimen	Implant	Width 1/2_max	Depth	Oxide	Depth + Oxide_thickness
1	He	910	1863	1515	3378
2	He + H	1020	1585	1511	3096
3	H	910	1926	1363	3289
4	H + He	1310	1646	1386	3032

	Co-implant	Single
Average	3064	3334
Stdev	45.3	62.9
% dev	1.5%	1.9%

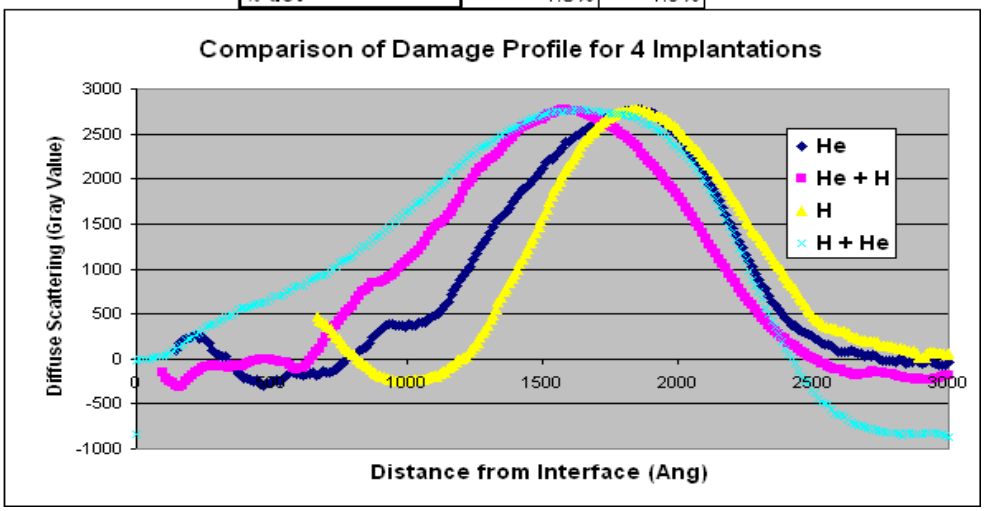

Figure 4

Damage Layer Structure:

Our goal in characterizing the structure of the damage layer was to get a size range for the texture within the layer. The method of getting power spectra ratios is sensitive to specimen thickness since overlapping "dots" act to wash out the spatial frequency information by blurring the texture. To show this, the analysis was done in two regions of the same image where overlap is of different prevalence. In Figure 5, Region 2 has had less erosion from ion-milling and is therefore thicker, as the presence of the oxide layer suggests.

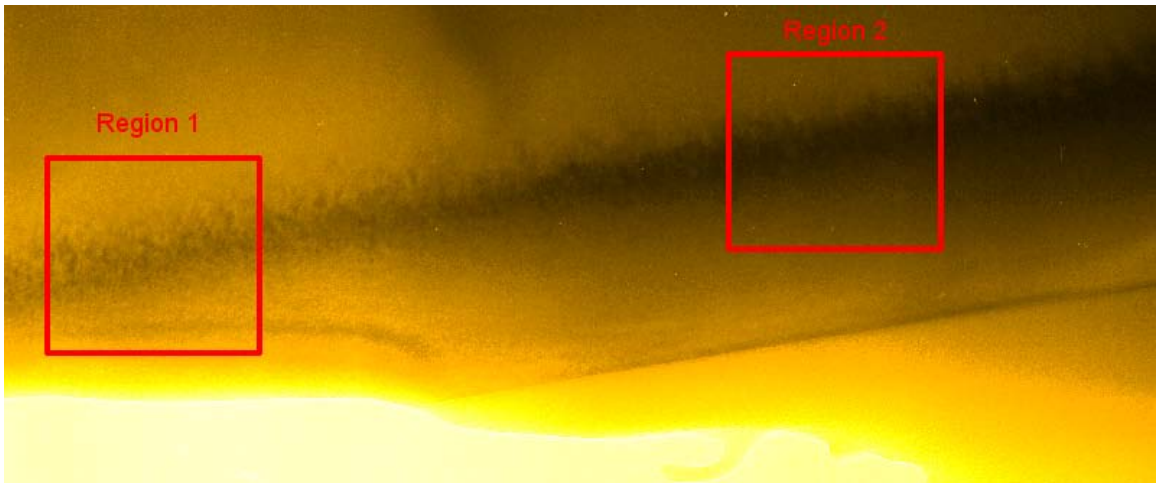

Figure 5

Figure 6 shows that the d-spacings in the 90-180 Angstrom range that are present in the thin region analysis are essentially washed out in the thicker region.

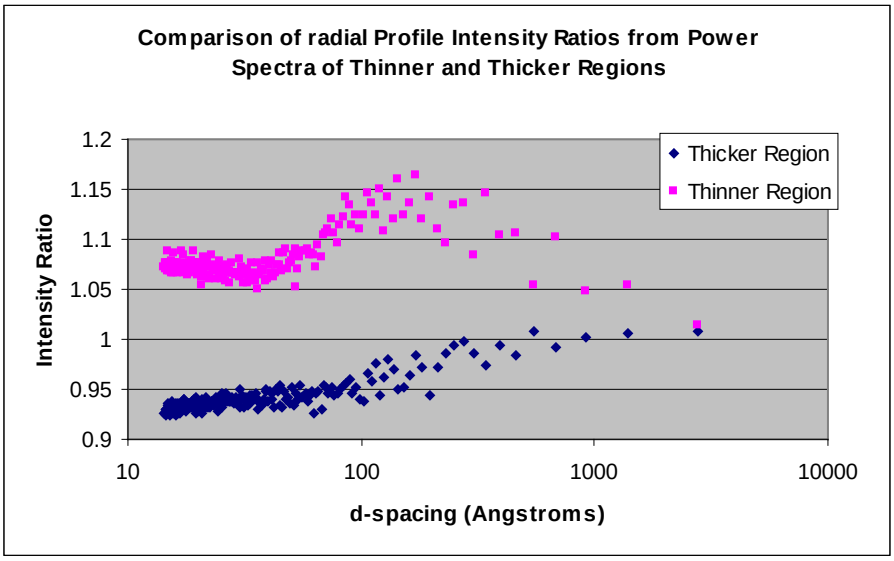

Figure 6

A digital darkfield routine was adopted to highlight the contribution of these size range fluctuations in the image. If there is contrast in what is thought to be the damage region, this gives us information concerning the structure that is independent of the band being dark in normal imaging conditions. A comparison of the direct-space and masked frequency-space image can be seen in Fig 7.

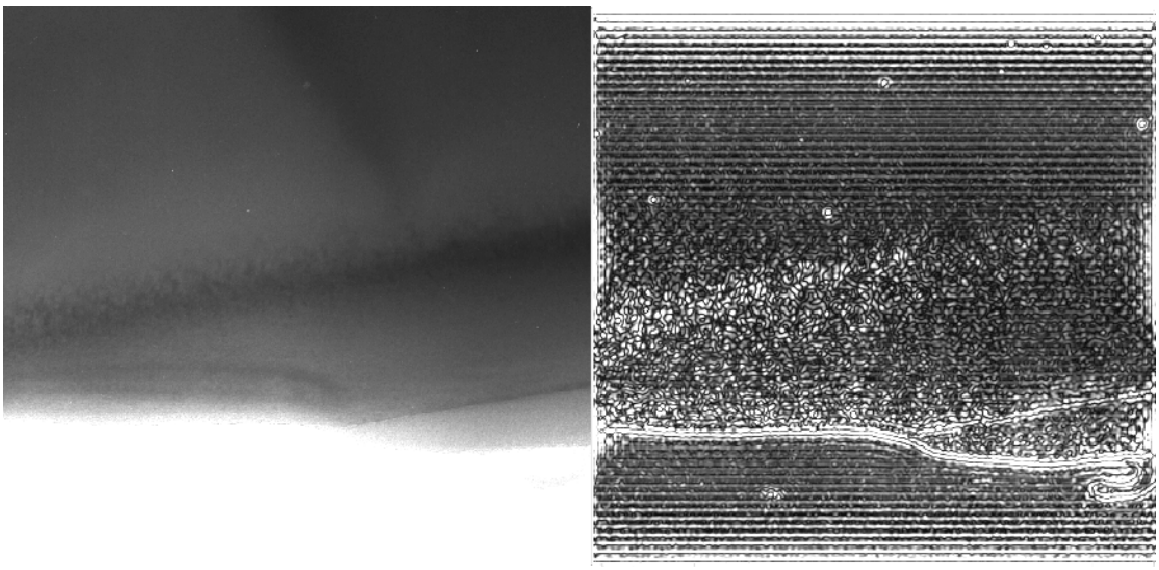

Figure 7

Despite the edge and ringing effects, there is clearly a higher intensity in the damage layer than in the bulk. We now not only have channeling contrast from displaced atoms,

but also contrast from intensity fluctuations in a particular size range. The feature of higher intensity in the thinner region is also consistent with the differences in power-spectrum ratios done above. The lower intensity of the damage layer in the thicker region shows that the size-fluctuations in the defined range are masked.

Discussion

Profile Data Stability and Features:

To check the consistency of the method, the profile analysis was done twice on the same image, but different locations, and also on two different images of the same specimen (Figure 8). In both cases, the widths were within about 15% of one another and can be attributed to differences in contrast features. The depths were more precise and within about 5%.

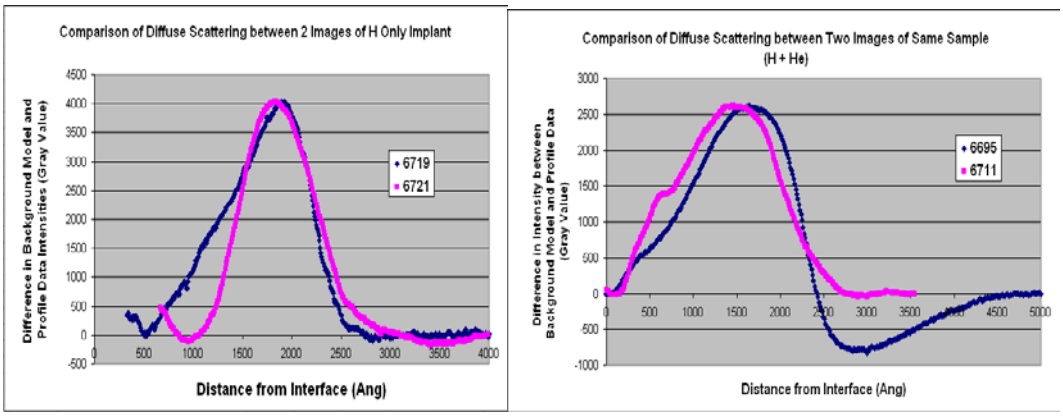

Figure 8

When the data (Figure 4) is sorted into co-implanted and single-species implanted specimens, the deviations from the average depth of the damage layer are within 2%. And though more data points are required to draw strong conclusions, this preliminary analysis suggests that co-implanted specimens leave a damage layer closer to the interface than single-implanted specimens. The full-width half-maximums also seems to be significantly larger for co-implanted specimens.

In some images, there was an intensity bump at the end of range. This may be explainable by strain contrast due to the pressure of the implanted gas. The literature[10] shows that the maximum of the helium profiles is about 30 nm deeper into the silicon than the maximum for the displaced atoms curve. The buildup of He could strain the lattice and give the contrast we observe, though the issue is complicated by interaction between the co-implanted species of He and H.

Conclusions

In the case of all four specimens, a dark band was observed that ran parallel to the interface and was at a depth that is consistent with the expectations of the damage layer location. The lack of BF/DF contrast complimentarity suggests that this is not typical diffraction contrast and the interpretation of channeling contrast due to a damaged lattice is consistent with the literature[10][11].

Though preliminary analysis of intensity profiles suggests that differences in implantation depths and full-width half-maximums can be measured, more data points are needed to reach quantitative conclusions. Since channeling contrast is the result of damage in an otherwise healthy crystal, intensity profiles in TEM images seems to be a good way of characterizing the damage layer.

The power spectra ratios between the damage layer and nearby healthy silicon show an intensity increase in fluctuations at the 90-180 Angstrom size range. When mapping fluctuations in the image at this size range with digital darkfield techniques, the damage layer shows a significantly higher intensity than the bulk.

References

[1]A H van Ommen and M P A Viegers. Microscopy of Semiconducting Materials Conference Proceedings (1987), pg 385.
[2]R. Sinclair. Electron Microscopy Society of America Conference Proceedings (1983), pg 130.
[3]F A Ponce, N M Johnson, et al. Microscopy of Semiconducting Materials Conference Proceedings (1987), pg 49.
[4]C. O. Jung, S. Visitserngtrakul, et al. Electron Microscopy Conference Proceedings (1990), Vol, 4: Material Sciences, pg 578.
[5]Ni Rushan and Lin Chenglu. Electron Microscopy Conference Proceedings (1990), Vol. 4: Material Sciences, pg 666.
[6]L. Mulestagno, R. Craven, and P. Fraundorf. JMSA Proceedings: Microscopy and Microanalysis (1995), 460.
[7]P. F. P. Fichtner, J. R. Kaschny, et al. Appl. Phys. Lett. **70**, 732 (1997).
[8]V. Raineri and M. Saggio. Appl. Phys. Lett. **71**, 1673 (1997).
[9]Aditya Agarwal, T. E. Haynes, et al, Appl. Phys. Lett. **72**, 1086 (1998).
[10]R. Tonini, F. Corni, S. Frabboni, G. Ottaviani & G. F. Cerofolini, J. Appl. Phys. **84**, 4802 (1998).
[11]Xinzhong Duo, Weili Liu, et al. J. Appl. Phys. D **34**, 5 (2001).
[12]N. Hueging, M. Luysberg, et al. Appl. Phys. Lett. **86**, 042112 (2005).
[13]K Johnson, X Lin, et al. Microscopy and Microanalysis Conference Proceedings (2007), pg CD786.